# Changing Hydrogen-Bond Structure during an Aqueous Liquid-Liquid Transition Investigated with Time-Resolved and Two-Dimensional Vibrational Spectroscopy

Bruijn, J.R.; van der Loop, T.H.; Woutersen, S.

DOI
10.1021/acs.jpclett.5b02861

Publication date
2016

Document Version
Final published version

Published in
The Journal of Physical Chemistry Letters

THE JOURNAL OF PHYSICAL CHEMISTRY Letters

Letter

pubs.acs.org/JPCL

# Changing Hydrogen-Bond Structure during an Aqueous Liquid–Liquid Transition Investigated with Time-Resolved and Two-Dimensional Vibrational Spectroscopy

Jeroen R. Bruijn, Tibert H. van der Loop, and Sander Woutersen*

Van 't Hoff Institute for Molecular Sciences (HIMS), University of Amsterdam, Science Park 904, 1098 XH Amsterdam, The Netherlands

Supporting Information

**ABSTRACT:** We investigate the putative liquid–liquid phase transition in aqueous glycerol solution, using the OD-stretch mode in dilute OD/OH isotopic mixtures to probe the hydrogen-bond structure. The conversion exhibits Avrami kinetics with an exponent of $n = 2.9 \pm 0.1$ (as opposed to $n = 1.7$ observed upon inducing ice nucleation and growth in the same sample), which indicates a transition from one liquid phase to another. Two-dimensional infrared (2D-IR) spectroscopy shows that the initial and final phases have different hydrogen-bond structures: the former has a single Gaussian distribution of hydrogen-bond lengths, whereas the latter has a bimodal distribution consisting of a broad distribution and a narrower, ice-like distribution. The 2D-IR spectrum of the final phase is identical to that of ice/glycerol at the same temperature. Combined with the kinetic data this suggests that the liquid–liquid transformation is immediately followed by a rapid formation of small (probably nanometer-sized) ice crystals.

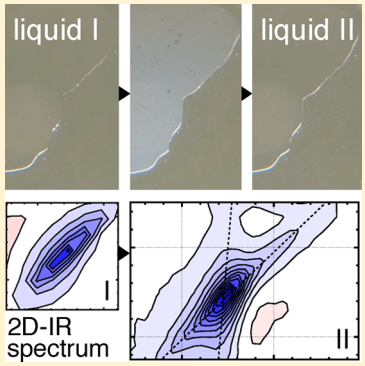


There are reasons to believe[1−7] that the anomalous properties of liquid water could be related to a phase transition between two different liquid states of water at a temperature far below the homogeneous nucleation temperature $T_{hom} \approx 235$ K. These two liquid states would correspond to the two different amorphous phases of water that exist below 135 K.[8,9] Because for $T > T_{hom}$ only one liquid phase is known to exist, the critical point at the end of the phase line between the two liquid phases would have to be at a temperature below $T_{hom}$. The divergence of the susceptibilities (expansion coefficient, compressibility, specific heat) at this critical point would explain the well-known anomalous temperature dependence of these susceptibilities in supercooled water.[10,11] Experimental evidence for the existence of two liquid states of water is difficult to obtain because the temperature at which the two liquid phases are believed to coexist is not experimentally accessible: it cannot be reached from the high-temperature side because of homogeneous nucleation at $T_{hom}$, and it cannot be reached from the low-temperature side by heating amorphous water because that spontaneously converts to ice at $T_x \approx 150$ K. The region between $T_x$ and $T_{hom}$ is therefore known as the "No man's land" of liquid water.

Thus, it seems impossible to observe the liquid–liquid phase transition of water. However, several approaches have been developed to deal with the problem of homogeneous nucleation and consequent freezing. Combined rapid cooling and ultrafast X-ray probing has made it possible to study liquid water at several K below $T_{hom}$ shortly before it freezes,[12−14] while the value of $T_x$ can be increased several K by pressure-annealing low-density amorphous water.[15] Freezing can be prevented altogether by confining water to volumes smaller than the critical nucleation size, and in confined systems evidence for liquid–liquid transitions has been observed,[16−19] but because of the strong interfacial interactions, the significance of these observations for bulk liquid water is unclear. Freezing can also be prevented by adding glycerol to water, and these experiments have shown evidence for a liquid–liquid phase transition in glycerol/water solution.[20,21] The molecular structure of the two observed phases is the subject of active debate.[5,20−25] Here, we use time-resolved infrared spectroscopy to study the kinetics of this phase transition and two-dimensional infrared spectroscopy to investigate the hydrogen-bond structures of the two phases. As a probe of the hydrogen-bond structure we use the linear and nonlinear response of the OD-stretch mode in dilute isotopic OD/OH mixtures[26] to prevent resonant coupling and energy transfer between OD groups.[27,28] The OD-stretch mode is a sensitive probe of hydrogen bonding in aqueous systems[29−33] because of the approximately linear relation between the OD-stretch frequency and the length of the OD···O hydrogen bond.[34]

Using the sample preparation procedure of ref 20, we reproduce the reported phase transition in our lab. We use an $x = 0.172$ glycerol/water mixture with an OD isotope fraction of 5%. Samples are prepared by putting a droplet between two $CaF_2$ windows separated by a ∼10 $\mu$m thick mylar spacer; the sample volume is sufficiently small that the squashed droplet

**Received:** December 23, 2015
**Accepted:** February 10, 2016
**Published:** February 18, 2016





DOI: 10.1021/acs.jpclett.5b02861
J. Phys. Chem. Lett. 2016, 7, 795−799

has no contact with the spacer. We find (see Supporting Information) that the OH and OD groups are distributed statistically over the glycerol and water molecules. We rapidly (10 K/min.) cool to 171 K and keep the temperature fixed at that value. Then, on a time scale of tens of minutes, a phase transition can be observed (visible to the naked eye, see Figure 1A), in which a new liquid phase (referred to as "liquid II" in the remainder) is formed as droplets in the initial liquid phase ("liquid I").[20,21] Upon completion of the phase transition, a new homogeneous phase is obtained, and the light scattering disappears (Figure 1A).

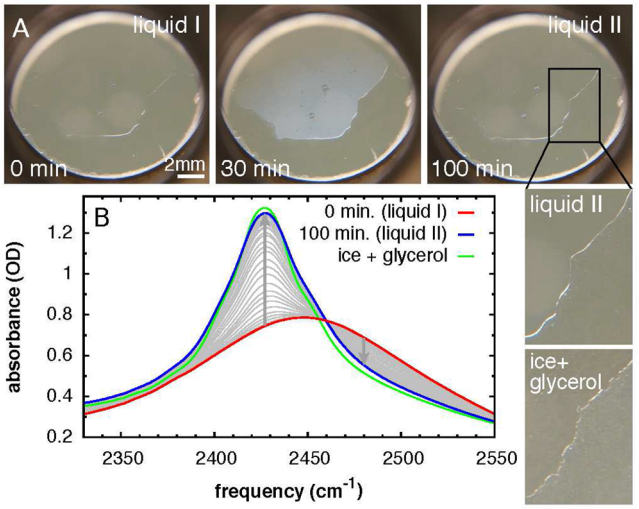


**Figure 1.** (A) Phase transition in $x$ = 0.172 glycerol–water mixture at 171 K. The close-ups highlight the interfaces of the liquid II phase and of ice/glycerol, prepared with the same sample (note that the shape of the squashed droplet remains the same). (B) Changing IR absorption spectrum during the transition from liquid I to liquid II. For comparison, the spectrum of ice in water/glycerol at the same temperature and composition is also shown.

To investigate the nature of the phase transition and the structure of the two phases, we measure the change in OD-stretch response during the phase transition. The $x$ = 0.172 glycerol/water solution can also undergo a transition to its thermodynamically most stable state, a suspension of small crystals in a glycerol-rich liquid phase (termed "ice/glycerol" in the remainder).[20,21,25] To compare the liquid–liquid phase transition with the formation of ice crystals, we also perform experiments in which we deliberately generate ice crystals by keeping the temperature at 195 K until ice nucleation and growth have occurred (a process that is easily visible, see Figure 1A) and subsequently cool to 171 K, the temperature at which the liquid–liquid transition is observed after rapid cooling. By comparing the infrared (IR) and two-dimensional IR (2D-IR) spectra of these samples at the same temperature, we can determine the difference in hydrogen-bond structure between liquid I, liquid II, and ice/glycerol.

Figure 1B shows the OD-stretch region of the sample as it transforms from liquid I to liquid II at 171 K. It should be noted that both HOD and glycerol-OD contribute to this absorption (in a water:glycerol ratio of 3.21:1). The IR spectrum of liquid I is a broad, approximately Gaussian band. The evolution from liquid I to liquid II is clearly visible, and the presence of an isosbestic point at 2459 $cm^{-1}$ indicates that there is a one-to-one conversion of one phase to another. The spectrum of liquid II consists of a narrow peak with broad wings. The center frequency of this peak (2427 $cm^{-1}$) is comparable to the OD-stretch frequency of ~2425 $cm^{-1}$ of dilute HDO:$H_2O$ ice at 171 K.[35] The spectrum of ice/glycerol (green curve in Figure 1B) is very similar to that of liquid II.

The time dependence of the IR spectrum can be used to probe the kinetics of the phase transition. In Figure 2 we show the time dependence of the fraction $F$ of liquid II, in a conventional (inset) and in an Avrami plot. The converted fraction is determined from the time-dependent absorbance $A(t)$ at 2427 $cm^{-1}$ as $F(t) = [A(t) - A(0)]/[A(\infty) - A(0)]$. For comparison, we also show the growth of the ice fraction observed during ice/glycerol formation. We find that in both cases, the time dependence of the fraction $F(t)$ of converted material can be well-described using the Avrami equation:[36,37]

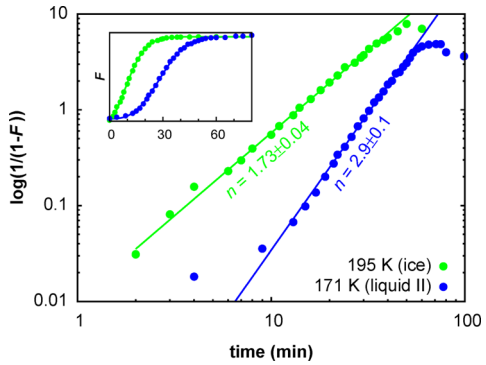


**Figure 2.** Kinetics of the phase transition at 195 K (ice formation) and 171 K (liquid–liquid transition) as determined from the IR data. The inset shows the fraction of converted mixture on a normal scale; the main plot uses rescaled axes according to Avrami kinetics. The curves are least-squares fits through the data points.

$$F(t) = 1 - \exp(-kt^n) \quad (1)$$

where $k$ is a constant dependent on the growth rate. $n$ is a constant (the Avrami exponent) determined by the dimensionality of the growing phase and the type of nucleation,[37] but it can also be influenced by the geometry (bulk or thin layer) of the sample.[38,39] If the phase transformation occurs according to eq 1, then a plot of $-\ln(1 - F)$ versus time on a double-logarithmic scale should be a straight line, as we observe. The value of $n$ depends on the nucleation and growth mechanism and the dimensionality of the sample. For instance, for spherical growth and a constant nucleation rate, we have $n$ = 4 in an unconfined sample geometry[37] and $n$ = 3 in a thin layer (quasi-2D growth).[38,39] From a least-squares fit of eq 1 to the data we obtain $n$ = 1.73 ± 0.04 for the ice growth, which is similar to the values of 1.51 (at 155 K) and 1.74 (at 153 K) observed previously for ice growth in a several micrometer thick layer of hyperquenched neat water[40] and to the value of 1.7 predicted from simulations at 180 K.[41] For the liquid–liquid transition, we obtain $n$ = 2.9 ± 0.1, the same value as observed previously for the liquid–liquid transition of a 10 $\mu$m thick layer of triphenyl phosphite.[38]

To investigate the molecular structure of the two phases in more detail we use 2D-IR spectroscopy. Figures 3 and 4 show the 2D-IR spectra of liquid I, liquid II, and ice/glycerol, all measured at 171 K. In the 2D-IR experiments, we resonantly excite the OD-stretch mode using a narrow-band pump pulse and measure the resulting change in absorption using a delayed


DOI: 10.1021/acs.jpclett.5b02861
J. Phys. Chem. Lett. 2016, 7, 795–799

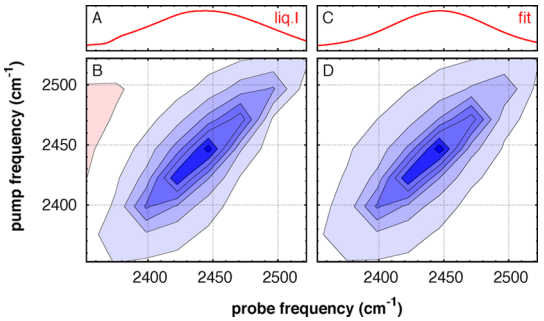


**Figure 3.** (A) FTIR and (B) 2D-IR spectrum of liquid I at 171 K. (D) Results of a least-squares fit of a Bloch line shape model to the data shown in panel B; (C) IR spectrum calculated using the parameters obtained from the fit to the 2D-IR data.

broad-band probe pulse, which is detected in a spectrally dispersed manner. By doing this for a series of pump frequencies, we obtain a 2D plot of the absorption change versus the pump and probe frequencies. In Figures 3 and 4 only the negative absorption change due to the bleach and stimulated emission of the $\nu_{OD} = 0 \rightarrow 1$ transition is observed because the $\nu_{OD} = 1 \rightarrow 2$ excited-state absorption is at a frequency outside the spectral range of the experiment.[42] Because liquid I exists only for several minutes before changing into liquid II (see inset of Figure 2), we have to scan the pump frequency quickly so that the spectral resolution along the $\nu_{pump}$ axis is lower for liquid I than for the other samples.

The 2D-IR response of liquid I (Figure 3B) is elongated along the diagonal, which indicates that the OD-stretch absorption band is inhomogeneously broadened.[43] The OD-stretch contributions of the glycerol and water molecules in the solution cannot be distinguished in the 2D-IR spectrum of liquid I. We find that we can quantitatively describe the response by a Bloch line shape, in which the OD-groups all have the same Lorentzian line shape but centerfrequencies that are distributed according to a normal distribution. From a least-squares fit of this model[44] to the data (Figure 3D) we obtain the spectral parameters listed in Table 1. The uncertainties in the fit parameters as determined from the covariance matrix are underestimates because systematic errors are not taken into account.

Figure 4B shows the 2D-IR spectrum of liquid II. The small positive contribution at $(\nu_{probe}, \nu_{pump}) = (2450, 2410)$ cm$^{-1}$ is due to a temperature increase caused by partial vibrational relaxation during the pump–probe waiting time. As in the case

**Table 1. Spectral Parameters Obtained from Least-Squares Fits of a Single and Bimodal Bloch Model to the Data Shown in Figures 3 and 4[a]**

| parameter | liquid I | liquid II | ice/glycerol |
|---|---|---|---|
| $\nu_1^0$ (cm$^{-1}$) | 2447.2 ± 0.8 | 2428.8 ± 0.7 | 2427.7 ± 0.8 |
| $\sigma_1$ (cm$^{-1}$) | 35.2 ± 0.8 | 30.6 ± 2.2 | 29.6 ± 1.7 |
| $\nu_2^0$ (cm$^{-1}$) | | 2431.1 ± 0.3 | 2430.5 ± 0.3 |
| $\sigma_2$ (cm$^{-1}$) | | 7.5 ± 0.5 | 6.9 ± 0.4 |
| $\gamma$ (cm$^{-1}$) | 3.3 ± 0.2 | 3.5[b] | 3.3[b] |
| $A_1/(A_1 + A_2)$ | | 0.72 ± 0.02 | 0.67 ± 0.01 |

[a] $\gamma$ is the half-width at half-max of the Lorentzian lineshape, and the distribution of center frequencies, $\nu$, is given by $\exp[-(\nu - \nu^0)^2/2\sigma^2]$. The reported uncertainties are 1 standard deviation. $A_1/(A_1 + A_2)$ is the amplitude ratio of the two Bloch lineshapes. [b] These homogeneous line widths were kept fixed to their $T_1$-limited minimum[43] during the fit.

of liquid I, the slanted bleaching/stimulated emission in the 2D-IR spectrum reflects the spectral inhomogeneity of the sample. As opposed to liquid I, in liquid II the 2D spectrum consists of two distinct contributions (indicated by dotted lines in Figure 4B): one contribution that is elongated along the diagonal in a manner similar to that in liquid I and one contribution that is nearly vertically oriented, indicating much less spectral inhomogeneity. The spectrum can be described quantitatively (least-squares fit shown in Figure 4D) by a sum of two Bloch line shape functions; the spectral parameters obtained from a least-squares fit are listed in Table 1. The 2D-IR spectrum of ice/glycerol is nearly identical to that of liquid II; the only (and small) difference is the relative intensities of the spectrally narrow and broad components. The narrow component in the ice/glycerol spectrum has a width and center frequency similar to that of ice Ih at this temperature,[42] and we can therefore assign this component to the ice crystals in the sample and the broad spectral component to the remaining glycerol-rich water surrounding the ice crystals. In this latter phase, the OD-stretch modes of water and glycerol again cannot be separated, as in liquid I.

The similarity of the 2D-IR spectra of liquid II and ice/glycerol suggests that liquid II consists of ice crystallites embedded in a glycerol-rich liquid. Evidence for the presence of nanometer-sized ice crystals in liquid II was observed in its X-ray diffraction,[20,21] and calorimetric and dielectric-relaxation measurements also indicate freezing during the phase transition.[25] However, the Avrami exponent of $n = 2.9 \pm 0.1$ (Figure 2) seems to indicate a transformation of one liquid

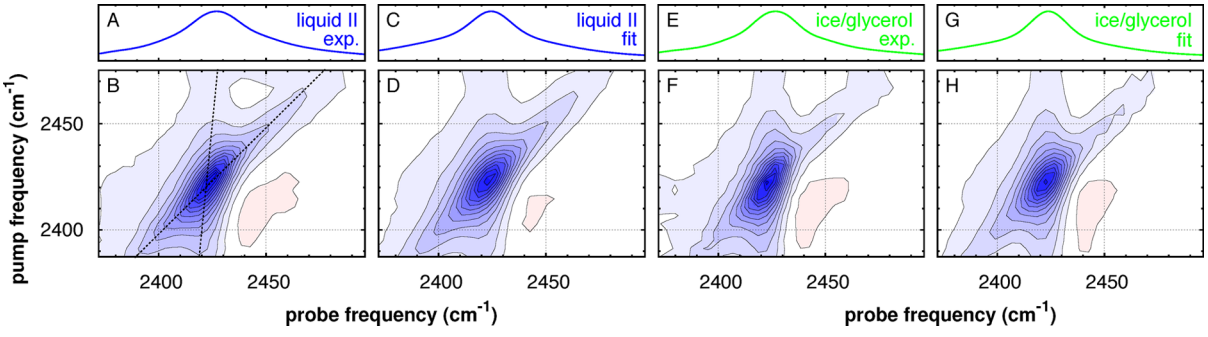


**Figure 4.** (A) FTIR and (B) 2D-IR spectrum of liquid II at 171 K. (C, D) Calculated spectra using the fit parameters of Table 1. (E) FTIR and (F) 2D-IR spectrum of liquid II ice/glycerol at 171 K. (G, H) Calculated spectra using the fit parameters of Table 1. The dotted lines are guides to the eye.



DOI: 10.1021/acs.jpclett.5b02861
J. Phys. Chem. Lett. 2016, 7, 795–799

phase into another[37] rather than aborted crystallization.[45] In addition, Raman-microscopy measurements show that the droplets of liquid II observed during the transition have the same composition as liquid I.[24] The situation might be similar to the liquid−liquid transition in aqueous LiCl solution, which involves the formation of domains of low-density liquid water (with local tetrahedral coordination) from which the solute is expelled to form a surrounding solute-rich high-density water phase.[46−50] In the present case, this liquid phase-separated state would have to be a short-lived intermediate because the IR and 2D-IR spectra of the ice-like component of liquid II are similar to those of crystalline ice[31,35,51] and very different from those of (isotope-diluted) low-density amorphous water.[52−54] This is possible if the formation of the intermediate state is much slower than its subsequent conversion to ice/glycerol; in that case, the observed conversion kinetics can be liquidlike (as the Avrami exponent indicates), even though (submicrometer) ice crystals are formed (as is observed in the 2D-IR spectrum). Because the temperature of 171 K is well above the glass temperature, such a rapid conversion into ice is perhaps not unlikely (and it might be slowed or even prevented if the liquid−liquid transition could be observed at much lower temperature). A mechanism along these lines has already been hinted at[5,23] and would be similar to the recently investigated crystallization of $CaSO_4$ in water, which occurs via a precursor state with dense liquid droplets that rapidly (within ∼1 s) convert to the crystalline state.[55]

To summarize, 2D-IR spectroscopy provides direct access to the hydrogen-bond structures of the two low-temperature liquid phases of water/glycerol and reveals that they are fundamentally different. The bimodal hydrogen-bond distribution of liquid II, which is very similar to that of ice/glycerol, suggests that this liquid consists of nanometer-sized ice crystals embedded in a glycerol-rich water matrix. We believe our results demonstrate that 2D-IR spectroscopy can be a valuable tool for investigating liquid−liquid phase transitions in hydrogen-bonded liquids, and we are currently applying this method to liquid−liquid transitions in aqueous salt solutions.[56]

## ■ ASSOCIATED CONTENT

### Supporting Information

The Supporting Information is available free of charge on the ACS Publications website at DOI: 10.1021/acs.jpclett.5b02861.

Experimental details and verification of OD/OH exchange between water and glycerol. (PDF)

## ■ AUTHOR INFORMATION


### Corresponding Author

*E-mail: s.woutersen@uva.nl. Phone: +31 (0)20 525 7091. Fax: +31 (0)20 525 6965.


### Notes

The authors declare no competing financial interest.

## ■ ACKNOWLEDGMENTS

The authors thank Michiel Hilbers for technical support, and Hajime Tanaka, Austen Angell, and Peter Hamm for valuable suggestions and comments. This work is part of the research programme of the Foundation for Fundamental Research on Matter (FOM), which is part of The Netherlands Organisation for Scientific Research (NWO).

## ■ REFERENCES


(1) Poole, P. H.; Sciortino, F.; Essmann, U.; Stanley, H. E. Phase behavior of metastable water. *Nature* **1992**, *360*, 324−328.

(2) Angell, C. A.; Bressel, R. D.; Hemmati, M.; Sare, E. J.; Tucker, J. C. Water and its anomalies in perspective: tetrahedral liquids with and without liquid-liquid phase transitions. *Phys. Chem. Chem. Phys.* **2000**, *2*, 1559−1566.

(3) Sastry, S.; Angell, C. A. Liquid-liquid phase transition in supercooled silicon. *Nat. Mater.* **2003**, *2*, 739−743.

(4) Holten, V.; Anisimov, A. Entropy-driven liquid-liquid separation in supercooled water. *Sci. Rep.* **2012**, *2*, 713.

(5) Angell, C. A. Supercooled liquids: Clearing the water. *Nat. Mater.* **2012**, *11*, 362−364.

(6) Angell, C. A. Two phases? *Nat. Mater.* **2014**, *13*, 673−675.

(7) Nilsson, A.; Pettersson, L. G. M. The structural origin of anomalous properties of liquid water. *Nat. Commun.* **2015**, *6*, 8998.

(8) Mishima, O.; Calvert, L. D.; Whalley, E. An apparently first-order transition between two amorphous phases of ice induced by pressure. *Nature* **1985**, *314*, 76−78.

(9) Seidl, M.; Amann-Winkel, K.; Handle, P. H.; Zifferer, G.; Loerting, T. From parallel to single crystallization kinetics in high-density amorphous ice. *Phys. Rev. B: Condens. Matter Mater. Phys.* **2013**, *88*, 174105.

(10) Zheleznyi, B. V. The density of supercooled water. *Russ. J. Phys. Chem.* **1969**, *43*, 1311−1312.

(11) Rasmussen, D. H.; MacKenzie, A. P.; Angell, C. A.; Tucker, J. C. Anomalous heat capacities of supercooled water and heavy water. *Science* **1973**, *181*, 342−344.

(12) Sellberg, J. A.; Huang, C.; McQueen, T. A.; Loh, N. D.; Laksmono, H.; Schlesinger, D.; Sierra, R. G.; Nordlund, D.; Hampton, C. Y.; Starodub, D.; et al. Ultrafast X-ray probing of water structure below the homogeneous ice nucleation temperature. *Nature* **2014**, *510*, 381−384.

(13) Sellberg, J. A.; McQueen, T. A.; Laksmono, H.; Schreck, S.; Beye, M.; DePonte, D. P.; Kennedy, B.; Nordlund, D.; Sierra, R. G.; Schlesinger, D.; et al. X-ray emission spectroscopy of bulk liquid water in no-man's land. *J. Chem. Phys.* **2015**, *142*, 044505.

(14) Laksmono, H.; McQueen, T. A.; Sellberg, J. A.; Loh, N. D.; Huang, C.; Schlesinger, D.; Sierra, R. G.; Hampton, C. Y.; Nordlund, D.; Beye, M.; et al. Anomalous behavior of the homogeneous ice nucleation rate in no-man's land. *J. Phys. Chem. Lett.* **2015**, *6*, 2826−2832.

(15) Seidl, M.; Fayter, A.; Stern, J. N.; Zifferer, G.; Loerting, T. Shrinking water's no man's land by lifting its low-temperature boundary. *Phys. Rev. B: Condens. Matter Mater. Phys.* **2015**, *91*, 144201.

(16) Bergman, R.; Swenson, J. Dynamics of supercooled water in confined geometry. *Nature* **2000**, *403*, 283−286.

(17) Koga, K.; Gao, G. T.; Tanaka, H.; Zeng, X. C. Formation of ordered ice nanotubes inside carbon nanotubes. *Nature* **2001**, *412*, 802−805.

(18) Mallamace, F.; Broccio, M.; Corsaro, C.; Faraone, A.; Majolino, D.; Venuti, V.; Liu, L.; Mou, C. Y.; Chen, S. H. Evidence of the existence of the low-density liquid phase in supercooled, confined water. *Proc. Natl. Acad. Sci. U. S. A.* **2007**, *104*, 424−428.

(19) Han, S.; Choi, M. Y.; Kumar, P.; Stanley, H. E. Phase transitions in confined water nanofilms. *Nat. Phys.* **2010**, *6*, 685−690.

(20) Murata, K.; Tanaka, H. Liquid-liquid transition without macroscopic phase separation in a water-glycerol mixture. *Nat. Mater.* **2012**, *11*, 436−443.

(21) Murata, K.; Tanaka, H. General nature of liquid-liquid transition in aqueous organic solutions. *Nat. Commun.* **2013**, *4*, 2844.

(22) Limmer, D. T.; Chandler, D. The putative liquid-liquid transition is a liquid-solid transition in atomistic models of water. *J. Chem. Phys.* **2011**, *135*, 134503.

(23) Limmer, D. T.; Chandler, D. Corresponding states for mesostructure and dynamics of supercooled water. *Faraday Discuss.* **2014**, *167*, 485−498.




DOI: 10.1021/acs.jpclett.5b02861
*J. Phys. Chem. Lett.* 2016, 7, 795−799

(24) Tanaka, H. Importance of many-body orientational correlations in the physical description of liquids. *Faraday Discuss.* **2014**, *167*, 9–76.
(25) Popov, I.; Greenbaum, A.; Sokolov, A. P.; Feldman, Y. The puzzling first-order phase transition in water-glycerol mixtures. *Phys. Chem. Chem. Phys.* **2015**, *17*, 18063–18071.
(26) Water and glycerol exhibit mutual OH/OD exchange, see Supporting Information.
(27) Cowan, M. L.; Bruner, B. D.; Huse, N.; Dwyer, J. R.; Chugh, B.; Nibbering, E. T. J.; Elsaesser, T.; Miller, R. J. D. Ultrafast memory loss and energy redistribution in the hydrogen bond network of liquid $H_2O$. *Nature* **2005**, *434*, 199–202.
(28) Panman, M. R.; Shaw, D. J.; Ensing, B.; Woutersen, S. Local orientational order in liquids revealed by resonant vibrational energy transfer. *Phys. Rev. Lett.* **2014**, *113*, 207801.
(29) Loparo, J. J.; Roberts, S. T.; Tokmakoff, A. Multidimensional infrared spectroscopy of water. II. Hydrogen bond switching dynamics. *J. Chem. Phys.* **2006**, *125*, 194522.
(30) Auer, B. M.; Skinner, J. L. IR and Raman spectra of liquid water: Theory and interpretation. *J. Chem. Phys.* **2008**, *128*, 224511.
(31) Li, F.; Skinner, J. L. Infrared and Raman line shapes for ice Ih. I. Dilute HOD in $H_2O$ and $D_2O$. *J. Chem. Phys.* **2010**, *132*, 204505.
(32) Nicodemus, R. A.; Ramasesha, K.; Roberts, S. T.; Tokmakoff, A. Hydrogen bond rearrangements in water probed with temperature-dependent 2DIR. *J. Phys. Chem. Lett.* **2010**, *1*, 1068–1072.
(33) Perakis, F.; Hamm, P. Two-dimensional infrared spectroscopy of supercooled water. *J. Phys. Chem. B* **2011**, *115*, 5289–5293.
(34) Novak, A. Hydrogen Bonding in Solids. Correlation of Spectroscopic and Crystallographic Data. *Struct. Bonding (Berlin)* **1974**, *18*, 177–216.
(35) Ford, T. A.; Falk, M. Hydrogen bonding in water and ice. *Can. J. Chem.* **1968**, *46*, 3579–3586.
(36) Avrami, M. Kinetics of Phase Change. II Transformation Time Relations for Random Distribution of Nuclei. *J. Chem. Phys.* **1940**, *8*, 212–224.
(37) Papon, P.; Leblond, J.; Meijer, P. H. E. *The Physics of Phase Transitions: Concepts and Applications*; Springer: Berlin, 2002.
(38) Kurita, R.; Tanaka, H. Kinetics of the liquid-liquid transition of triphenyl phosphite. *Phys. Rev. B: Condens. Matter Mater. Phys.* **2006**, *73*, 104202.
(39) Kurita, R.; Tanaka, H. Phase-ordering kinetics of the liquid-liquid transition in single-component molecular liquids. *J. Chem. Phys.* **2007**, *126*, 204505.
(40) Hage, W.; Hallbrucker, A.; Mayer, E.; Johari, G. P. Crystallization kinetics of water below 150 K. *J. Chem. Phys.* **1994**, *100*, 2743–2747.
(41) Moore, E. B.; Molinero, V. Ice crystallization in water's no-man's land. *J. Chem. Phys.* **2010**, *132*, 244504.
(42) Perakis, F.; Widmer, S.; Hamm, P. Two-dimensional infrared spectroscopy of isotope-diluted ice Ih. *J. Chem. Phys.* **2011**, *134*, 204505.
(43) Hamm, P.; Zanni, M. *Concepts and Methods of 2D Infrared Spectroscopy*; Cambridge University Press: Cambridge, 2011.
(44) The 1.2 ps pump–probe delay is comparable to the ~1 ps $v = 1$ lifetime of the OD-stretch mode. OD-stretch modes that are no longer in the $v = 1$ state do not contribute to the stimulated emission and bleach, but their vibrational relaxation causes a small local increase in temperature, which causes an absorption change that also contributes to the observed signals. We take this thermal contribution into account by adding the thermally equilibrated spectrum (measured separately by recording a 2D spectrum at long delay time) to the fit function, treating the amplitude of this contribution as a fit parameter.
(45) Mosses, J.; Syme, C. D.; Wynne, K. Order Parameter of the Liquid-Liquid Transition in a Molecular Liquid. *J. Phys. Chem. Lett.* **2015**, *6*, 38–43.
(46) Angell, C. A.; Sare, E. J. Liquid-Liquid Immiscibility in Common Aqueous Salt Solutions at Low Temperatures. *J. Chem. Phys.* **1968**, *49*, 4713–4714.
(47) Angell, C. A. Water and its anomalies in perspective: tetrahedral liquids with and without liquid-liquid phase transitions. *Chem. Rev.* **2002**, *102*, 2627–2660.
(48) Mishima, O. Application of polyamorphism in water to spontaneous crystallization of emulsified $LiCl/H_2O$ solution. *J. Chem. Phys.* **2005**, *123*, 154506.
(49) Mishima, O. Phase separation in dilute $LiCl\text{-}H_2O$ solution related to the polyamorphism of liquid water. *J. Chem. Phys.* **2007**, *126*, 244507.
(50) Le, L.; Molinero, V. Nanophase segregation in supercooled aqueous solutions and their glasses driven by the polymorphism of water. *J. Phys. Chem. A* **2011**, *115*, 5900–5907.
(51) Perakis, F.; Hamm, P. Two-dimensional infrared spectroscopy of neat ice Ih. *Phys. Chem. Chem. Phys.* **2012**, *14*, 6250–6256.
(52) Bergren, M. S.; Schuh, D.; Sceats, M. G.; Rice, S. A. The OH stretching region infrared spectra of low density amorphous solid water and polycrystalline ice Ih. *J. Chem. Phys.* **1978**, *69*, 3477–3482.
(53) Shalit, A.; Perakis, F.; Hamm, P. Two-Dimensional Infrared Spectroscopy of Isotope-Diluted Low Density Amorphous Ice. *J. Phys. Chem. B* **2013**, *117*, 15512–15518.
(54) Tainter, C. J.; Shi, L.; Skinner, J. L. Structure and OH-stretch spectroscopy of low- and high-density amorphous ices. *J. Chem. Phys.* **2014**, *140*, 134503.
(55) Shahidzadeh, N.; Schut, M. F. L.; Desarnaud, J.; Prat, M.; Bonn, D. Salt stains from evaporating droplets. *Sci. Rep.* **2015**, *5*, 10335.
(56) Zhao, Z.; Angell, C. A. Apparent first-order liquid-liquid transition with pre-transition density anomaly, in water-rich ideal solutions. *Angew. Chem., Int. Ed.* **2016**, *55*, 2474–2477.


DOI: 10.1021/acs.jpclett.5b02861
*J. Phys. Chem. Lett.* 2016, 7, 795–799